RESEARCH ARTICLE

# Functionalized Cyclic Poly(α-Hydroxy Acids) via Controlled Ring-Opening Polymerization of *O*-Carboxyanhydrides

Ziyu Huo,[a] Xiaoyu Xie,[a] Nadim Mahmud,[b] Joshua C. Worch,[b] and Rong Tong* [a]

[a] Z. Huo, X. Xie, Prof. Dr. R. Tong
Department of Chemical Engineering, Virginia Polytechnic Institute and State University,
635 Prices Fork Road, Blacksburg, Virginia, 24061, United States
E-mail: rtong@vt.edu

[b] N. Mahmud, Prof. Dr. J. C. Worch
Department of Chemistry, Virginia Polytechnic Institute and State University,
1040 Drillfield Drive, Blacksburg, Virginia, 24061, United States

Supporting information for this article is given via a link at the end of the document

**Abstract:** Linear poly(α-hydroxy acids) are important degradable polymers, and they can be efficiently prepared by ring-opening polymerization of *O*-carboxyanhydrides with pendant functional groups. However, attempts to prepare cyclic poly(α-hydroxy acids) have been plagued by side reactions, including epimerization and uncontrolled intramolecular chain transfers or termination, that prevent the synthesis of high-molecular-weight stereoregular cyclic polyesters. Herein we report a scalable method for the synthesis of high-molecular-weight (>100 kDa) stereoregular functionalized cyclic poly(α-hydroxy acids) by means of controlled polymerization of *O*-carboxyanhydrides using a catalytic system consisting of a lanthanum complex with a sterically bulky ligand and a manganese silylamide. Additionally, using this system, we could readily prepare cyclic block poly(α-hydroxy acids) by means of sequential addition of *O*-carboxyanhydrides. The obtained cyclic polyesters and their cyclic block copolyesters exhibit distinctive physicochemical properties—including elevated phase transition temperature, improved toughness and reduced viscosity—compared to their linear counterparts.

## Introduction

The topology of polymers markedly affects their material properties.[1] Cyclic polymers—which have a unique topology without chain ends—exhibit various properties that are distinct from those of their linear analogues, including lower hydrodynamic volumes and radii, higher glass transition temperatures ($T_g$), and lower intrinsic viscosities ($\eta$).[2] Historically, petrochemical-based cyclic polymers, such as polyolefins, polyacrylates, and polyacetylenes, have been synthesized via well-established ring-expansion polymerization chemistry whereby the monomers are inserted into a growing ring. Notably, because of incomplete cyclization, intramolecular macrocyclization reactions of linear precursors at low concentrations cannot be scaled up.[2c, 3] Ring-expansion polymerization catalysts such as cyclic ruthenium complexes[4] and Lewis pair systems[5] efficiently produce cyclic polymers with molecular weights (MWs) of >100 kDa, some of which are being tested as lubricants or semiconducting materials for potential industrial applications.[6] In contrast, less work has been done on degradable cyclic polymers, particularly cyclic polyesters.[7]

Aliphatic polyesters derived from renewable resources show promise as recyclable, biodegradable, and biocompatible materials.[8] Controlled ring-expansion polymerization of cyclic monomers to produce cyclic polyesters—regardless of whether zwitterionic initiators[9] or metal complexes[10] are used—is often plagued by side reactions such as linear chain propagation,[7a] intramolecular chain transfer or termination,[10a, 10b, 11] and epimerization.[9, 12] Despite extensive work on methods for preparing cyclic poly(lactic acid) (*c*-PLA),[9-10] synthesis of cyclic PAHAs with high MWs (>100 kDa) and narrow MW distributions ($Đ$ < 1.2) remains a challenge (Figure 1A). For example, organotin catalysts can produce high-MW *c*-PLAs (165 kDa), but the MW distributions are large ($Đ$ = 1.8–8.7).[13] The polymerizations of L-lactide using *N*-heterocyclic carbenes produce epimerized *c*-PLAs with MWs of <30 kDa.[12a] Cerium(III) complexes have been shown to produce high-MW *c*-PLAs (~ 250 kDa) with large $Đ$ values (~ 1.5–1.8),[14] and a recently discovered air-stable indium(III) complex quantitatively produces high-MW *c*-PLAs (>400 kDa) with relatively broad MW distributions ($Đ$ ~ 1.2–1.5).[15] Additionally, methods for the formation of cyclic polyesters with pendant functional groups remain underexplored. Ring-opening polymerization (ROP) of *O*-carboxyanhydrides (OCAs),[16] a class of five-membered-ring monomers derived from amino acids, produces only low-MW cyclic poly(α-hydroxy acids) (PAHAs) with epimerization (Figure 1B).[12b, 17] Moreover, only one example of sequential addition of cyclic monomers to produce cyclic block copolyesters has been reported (MW < 40 kDa, $Đ$ ~ 1.4; Figure 1C),[18] in strong contrast to the innumerable reports on the synthesis of linear block copolyesters.[19] These synthetic difficulties have hampered exploration of the specific properties of cyclic functionalized polyesters with the goal of expanding their applications. Herein we present a method for controlled ROP of OCAs to prepare functionalized cyclic PAHAs with MWs of >100 kDa, $Đ$ values of <1.2, and no epimerization (Figure 1D). A particularly notable aspect of the method is that it enabled one-pot sequential addition of OCAs to prepare cyclic block copolyesters.

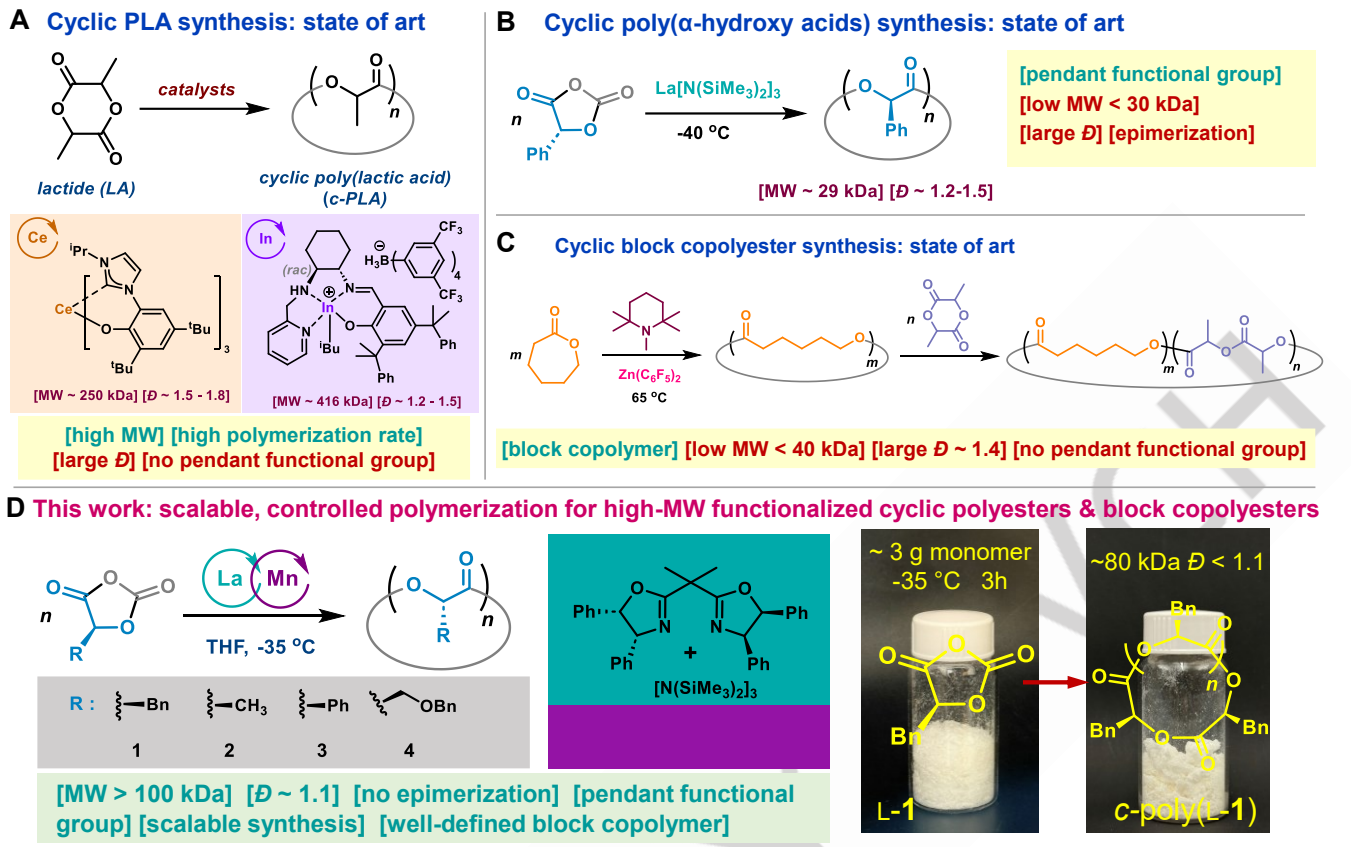


**Figure 1.** Strategies for synthesis of high-MW functionalized cyclic PAHAs and their block copolymers. (A) Synthesis of high-MW *c*-PLA. (B) Synthesis of functionalized cyclic PAHAs using a lanthanum complex. (C) Synthesis of cyclic block copolyesters by sequential addition of lactones. (D) Scalable, controlled ROP of OCAs with lanthanum/manganese complexes to afford high-MW functionalized cyclic polyesters and their block copolymers (this work). The pros and cons of various synthetic strategies are indicated in green and red, respectively.

## Results and Discussion

### Identification of Catalysts for Controlled ROP of OCAs to Afford Cyclic Polyesters

Historically, La[N(SiMe$_3$)$_2$]$_3$ has been employed as a practical catalyst to produce cyclic polyesters, including ROP of γ-butyrolactone,[20] and ROP of OCAs to produce PAHAs [12b] (Figure 1B). In ROP of γ-butyrolactone, the resultant MWs were below 30 kDa with high *Đ*s > 1.5; and the ROP of ring-fused γ-butyrolactone yielded cyclic polymers with MWs less than 90 kDa and *Đ*s ~ 1.5.[20] Epimerization occurs in ROP of OCAs, preventing the synthesis of functionalized cyclic stereoregular PAHAs with MWs exceeding 30 kDa.[12b] The frequent back-biting cyclization observed during the enchainment[20a] is believed to contribute to the broad MW distribution and may also induce epimerization (Scheme 1A).

To mitigate undesired side reactions, we hypothesized that the outcome of controlled ROP to produce cyclic polymers could be improved by selecting appropriate ligands for the lanthanum complex. This approach aims to minimize epimerization[21] and modulate steric hindrance around the catalytic metal center, thereby avoiding undesired back-biting cyclization and chain transfer reactions (Scheme 1B).[22] We posit that a sterically confined active lanthanum center would facilitate rapid enchainment, minimizing interruption by side reactions, thus narrowing MW distributions and maintaining cyclic structures during the enchainment. To further expedite enchainment, we use redox-active metal silylamides that promote decarboxylation during ROP of OCAs, which will enhance the production of high-MW cyclic PAHAs.[23] Notably, the selection of ligands has been previously utilized to control cyclic polymers' microstructures in the ROP of lactide[24] and thiolactone,[25] and the purpose of using ligands in these instances differs from our hypothesis.

**Scheme 1**. (A) Back-biting side reactions in cyclic PAHA synthesis. (B) Proposed strategy to mitigate such side reactions.

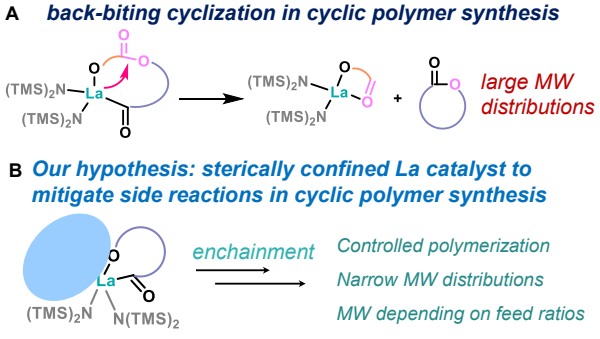

To test our hypothesis, we initially focused on ROP of L-**1** with the goal of identifying the optimal polymerization catalysts for production of cyclic poly(L-**1**) (*c*-poly(L-**1**)) at −35 ° C ([L-**1**]/[La] = 300/1, [L-**1**] = 0.392 M). We were pleased to confirm that the activity of La[N(SiMe$_3$)$_2$]$_3$ for producing cyclic polymers was superior to the activities of cerium or yttrium silylamides (Table S1, entry 1). In contrast, the use of La[N(SiHMe$_2$)$_2$]$_3$·(THF)$_2$ resulted in the formation of linear poly(L-**1**) (*l*-poly(L-**1**), entry 2). Consistent with the results of our previous study,[23] the combination of redox-active Mn[N(SiMe$_3$)$_2$]$_2$ (**Mn-1**) with La[N(SiMe$_3$)$_2$]$_3$ increased the MW of the obtained *c*-poly(L-**1**) (Table S2, entry 2). After extensive screening of ligands for the La[N(SiMe$_3$)$_2$]$_3$ complex (Table S3; analysis of catalyst ligand features in Supporting information Section S6), we found the optimal combination that consisted of a $C_2$-symmetric bis(oxazoline) ligand with the lanthanum silylamide complex (this in situ–prepared mixture is designated **La-1**) and **Mn-1**, which resulted in efficient polymerization that was complete within 0.5 h and afforded a polymer with a number-average MW ($M_n$) of 58.4 kDa, and a *Đ* of 1.04 (Table 1, entry 1). The *dn*/*dc* (refractive index increment) of the obtained polymer was 0.064, which is markedly lower than that of *l*-poly(L-**1**) (~ 0.10), suggesting a cyclic topology (see the size-exclusion chromatography [SEC] spectra in Figure S1). Notably, the addition of BnOH as an alcohol initiator for the ROP resulted in the formation of *l*-poly(L-**1**) (entry 2). As a control, the same experiment was performed without either **Mn-1** or **La-1**, and in both cases, monomer conversion was incomplete (entries 3 and 4). Using La[N(SiMe$_3$)$_2$]$_3$ without a ligand resulted in uncontrolled polymerization to afford a polymer with a lower $M_n$ and a larger *Đ* (entries 5 versus 1; also see Table S4, entries 4 versus 7), and the inclusion of a lanthanum complex in the catalytic system was essential for the formation of a cyclic polymer (comparing entries 1 and 5 with entry 4). The reaction could also be performed at −15 °C (entry 6); but at room temperature, monomer conversion was incomplete, and a linear topology was obtained (entry 7), indicating that a low reaction temperature was crucial for preventing side reactions. Note that reversing the chirality of the monomer (i.e., using D-**1** instead of L-**1**) had a negligible effect on the polymerization outcome (entry 8).

**Table 1**. Optimization of conditions for ROP of L-**1** to afford *c*-poly(L-**1**)[a]

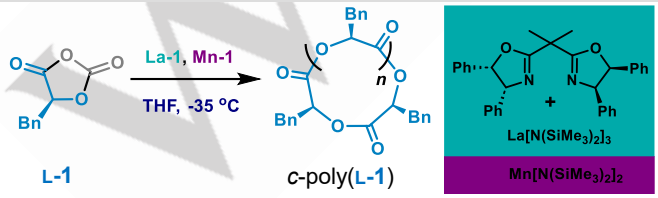


| Entry | Conditions | Time (h) | Conv. (%)[b] | $M_n$ (kDa)[c] | *Đ* [c] |
|---|---|---|---|---|---|
| 1 | as shown | 0.5 | 100 | 58.4 | 1.04 |
| 2[d] | add 1 equiv. BnOH | 0.5 | 100 | 30.1 | 1.12 |
| 3 | no **Mn-1** | 0.5 | 28.3 | 68.1 | 1.09 |
| 4[d] | no **La-1** | 0.5 | 24.8 | 41.9 | 1.17 |
| 5 | La[N(SiMe$_3$)$_2$]$_3$ instead of **La-1** | 0.5 | 100 | 34.4 | 1.14 |
| 6 | −15 °C | 0.5 | 100 | 57.7 | 1.02 |
| 7[d] | room temperature | 0.5 | 47.3 | 30.7 | 1.06 |
| 8 | D-**1** instead of L-**1** | 0.5 | 100 | 61.8 | 1.03 |
| 9 | reaction time, 3h | 3 | 100 | 57.6 | 1.03 |

[a] [L-**1**]/[**La-1**]/[**Mn-1**] = 300/1/1. The polymerizations were performed in a glovebox. [b] Monomer conversion (Conv.) was determined from the intensity of the Fourier transform infrared peak at 1805 cm$^{-1}$, which corresponds to the anhydride group of the OCA. [c] Determined by SEC. [d] A polymer with linear topology was obtained, as indicated by the *dn*/*dc* determined by SEC.

To confirm the cyclic nature of the obtained *c*-poly(L-**1**), we characterized it by using SEC (Figure 2A–C). Compared with *l*-poly(L-**1**) with a similar MW, our *c*-poly(L-**1**) had a smaller hydrodynamic volume (i.e., it eluted later; Figure 2A) and a lower radius of gyration ($R_g$, that is, the root mean square distance of the molecule's components from its center of gravity; Figure 2B). Additionally, a Mark–Houwink–Sakurada plot (i.e., log *η* versus log MW) showed that our *c*-poly(L-**1**) had a lower intrinsic viscosity than *l*-poly(L-**1**) ($\eta_{cyclic}/\eta_{linear}$ = 0.79; Figure 2C), confirming the circular topology of our polymer. Furthermore, the matrix-assisted laser desorption ionization (MALDI) mass spectrum of *c*-oligo(L-**1**) ([L-**1**]/[**La-1**] = 20/1) displayed peaks in multiples of 148.05 (decarboxylated L-**1** monomer) plus the ion mass, a result that indicates no end groups (Figure S2a). The single distribution of the peaks in MALDI spectrum confirmed the absence of linear byproducts. Such spectrum is distinct from that of a linear oligo(L-**1**) with BnO- end groups (Figure S2b).

Using the optimized conditions for polymerization of L-**1**, we found that the MW of *c*-poly(L-**1**) increased linearly as the initial L-**1**/La ratio was increased up to 450/1 ([**La-1**]/[**Mn-1**] = 1/1, [L-**1**] = 0.392 M; Figure 2D). At all the tested feed ratios, the *Đ* value of the *c*-poly(L-**1**) was less than 1.1 (Table S4, Figure S1c); and *dn*/*dc* showed little to no dependence on the feed ratio (Figure 2D), suggesting that the cyclic topology was maintained. Notably, no epimerization of the α-methine hydrogen was observed in the homodecoupled $^1$H NMR spectrum of *c*-poly(L-**1**) with a $M_n$ of 85.0 kDa (Figure S3). To confirm the living nature of the polymerization, we monitored the progress of the polymerization ([**La-1**]/[**Mn-1**] = 1/1, [L-**1**] = 0.392 M) and found that the MW of *c*-poly(L-**1**) was linearly correlated with L-**1** conversion; and at all the tested conversions, the polymer had a *Đ* of <1.1, and the *dn*/*dc* values did not vary substantially with conversion (Figure 2E). Notably, 2.5 h post-polymerization, the $M_n$ and *Đ* values of the obtained polymer remained nearly unchanged from those at polymerization completion (Table 1, entry 9), indicating that no undesired transesterification or back-biting cyclization[13a] occurred under the reaction conditions. Purification of *c*-poly(L-**1**) by washing with cold methanol did not affect the polymer's MW or *dn*/*dc* value (Table S4, entries 3 versus 6). Moreover, our La/Mn-mediated ROP of L-**1** at −35 °C exhibited first-order reaction kinetics

(Figures 2F and S4). These results collectively demonstrate that *c*-poly(L-**1**) retained its cyclic topology with a living reactive enchainment site during propagation.

Next we evaluated the generality of our La/Mn-mediated ROP strategy for polymerization of OCA monomers L-**2** – L-**4** (see Figure 1D for structures). The ROP of L-**2** proceeded smoothly with complete monomer conversions at initial L-**2**/La ratios up to 400/1 (Table 2, entry 1; Table S5; Figure S5), although high-MW *c*-poly(L-**2**) (>150 kDa) precipitated at −35 °C when the L-**2**/La ratio was increased to 500/1. Notably, MALDI mass spectrum of *c*-oligo(L-**2**) ([L-**1**]/[**La-1**] = 20/1) confirmed the only formation of circular topology in the polymerization (Figure S2c). Changing the α-carbon substituent from methyl (L-**2**) to phenyl (L-**3**) resulted in incomplete monomer conversion at an L-**3**/La feed ratio of 200/1 at a reaction temperature of −35 °C, even when the reaction time was extended to 30 h (Table 2, entry 2; Table S6). Although considerable epimerization of L-**3** was observed in a previously reported synthesis of *c*-poly(L-**3**),[12b] that did not occur in our system (Figure S6), suggesting that the ligands we incorporated helped to prevent epimerization.[21] Notably, MWs of *c*-poly(L-**2**) and *c*-poly(L-**3**) were also found linearly correlated with the monomer conversions; and the obtained polymers had *Đ*s of <1.1 at all of the tested conversions (Figures S5e and S6e). The ROP of L-**4**, which has a relatively bulky α-carbon substituent, showed a low monomer conversion at an L-**4**/La ratio of 200/1 even at −15 °C (Table S7, entry 3). Replacing **La-1** with **La-7** increased the monomer conversion (Table 2, entry 3) and no epimerization occurred (Figure S7). Importantly, like *c*-poly(L-**1**) (Figure 2A–C), all the obtained polymers had cyclic topologies, as determined by comparison of their SEC data (elution time, $R_g$, and $\eta$) with those for their linear counterparts (Figures S8–S10). Moreover, our cyclic *c*-poly(L-**1**) and *c*-poly(L-**2**) exhibited lower bulk rheological viscosities compared to their linear counterparts (Figure S11a-b), due to the reduced chain entanglement in cyclic polymers.

We used differential scanning calorimetry (DSC) to compare the thermal properties of the obtained cyclic PAHAs with the properties of linear analogues with similar MWs. Cyclic polymers *c*-poly(L-**1**), *c*-poly(L-**3**), and *c*-poly(L-**4**) all showed slightly higher $T_g$ values than their linear counterparts (Figure S11c, e, and f). Similarly, *c*-poly(L-**2**) exhibited a $T_m$ of 171.8 °C, which was higher than that of *l*-poly(L-**2**) (166.5 °C, Figure S11d). The stereocomplex polymer *c*-poly(*sc*-**1**), which is a 1/1 mixture of *c*-poly(L-**1**) and *c*-poly(D-**1**), had a slightly higher $T_g$ (51.8 °C) than that of *c*-poly(L-**1**) (49.6 °C, Figure S11c). Interestingly, the $T_m$ of another stereocomplex polymer, *c*-poly(*sc*-**2**), was substantially higher than that of *c*-poly(L-**2**) (214.8 °C versus 171.8 °C, Figure S11d).

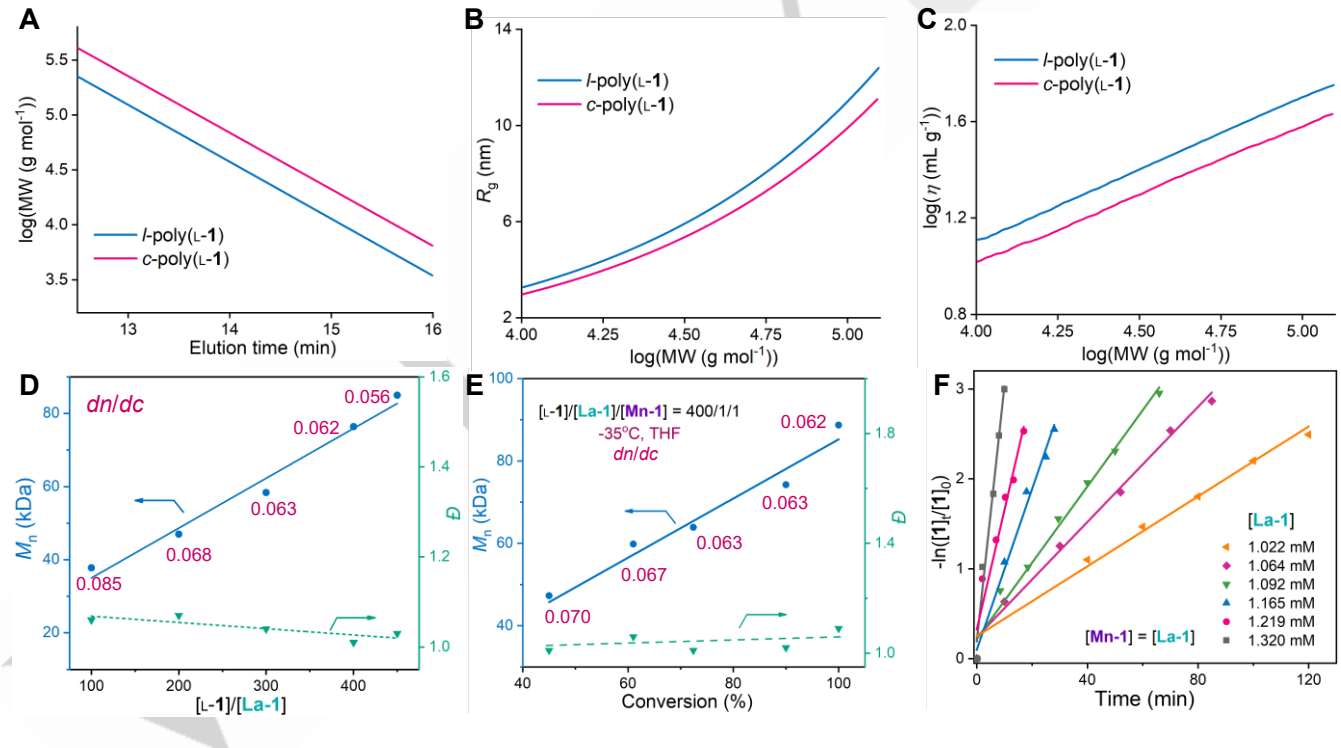


**Figure 2.** La/Mn-mediated controlled living polymerization of L-**1** to synthesize cyclic *c*-poly(L-**1**). (A) Plots of log MW versus SEC elution time, (B) plots of $R_g$ versus log MW, and (C) Mark–Houwink–Sakurada plots of log $\eta$ versus log MW for *l*-poly(L-**1**) and *c*-poly(L-**1**), as determined by SEC. (D) Plots of $M_n$ and *Đ* versus [L-**1**]/[**La-1**] ratio for *c*-poly(L-**1**) prepared at −35 °C ([**La-1**]/[**Mn-1**] = 1/1). (E) Plots of $M_n$ and *Đ* versus L-**1** conversion for *c*-poly(L-**1**) prepared at −35 °C ([L-**1**] = 0.392 M, [L-**1**]/[**La-1**]/[**Mn-1**] = 400/1/1). The *dn*/*dc* values of *c*-poly(L-**1**) in (D) and (E) are labelled in red. (F) Plots of L-**1** conversion versus time at various **La-1** concentrations ([L-**1**] = 0.392 M, [**La-1**]/[**Mn-1**] = 1/1).

**Table 2**. Controlled polymerization and block copolymerization of various OCA monomers to produce cyclic block PAHAs[a]

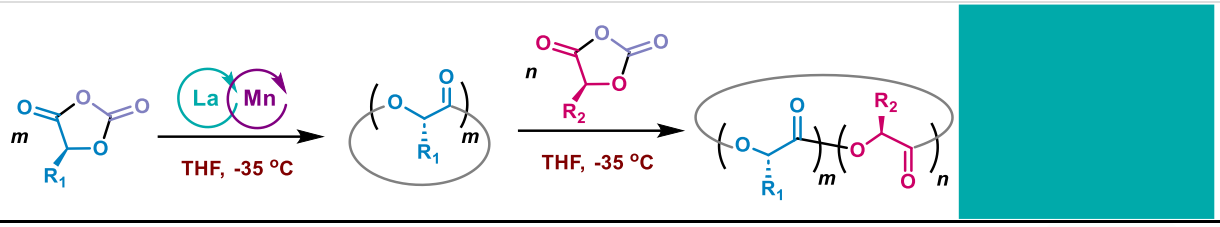


| Entry | Monomer | Catalyst | Feed ratio | Time | Conv. (%)[b] | $M_n$ ($M_n$-b1) (kDa)[c] | $Đ$ ($Đ$-b1)[c] |
|---|---|---|---|---|---|---|---|
| 1 | L-**2** | **La-1** | 400 | 4 h | 100 | 139.3 | 1.07 |
| 2 | L-**3** | **La-1** | 200 | 30 h | 85.0 | 78.8 | 1.06 |
| 3[d] | L-**4** | **La-7** | 100 | 2 h | 100 | 65.8 | 1.03 |
| 4 | L-**1**/L-**2** | **La-1** | 200/200 | 5 min/2 h | 100/100 | 87.0 (47.0) | 1.03 (1.07) |
| 5 | L-**2**/L-**1** | **La-1** | 200/200 | 5 min/3 h | 100/100 | 91.1 (51.8) | 1.03 (1.07) |
| 6[d] | L-**1**/L-**4** | **La-7** | 100/100 | 1 min/20 h | 100/82.4 | 69.9 (37.8) | 1.06 (1.06) |
| 7[d] | L-**2**/L-**4** | **La-7** | 200/100 | 15 min/12 h | 100/70.0 | 75.2 (51.8) | 1.07 (1.07) |
| 8[d] | L-**4**/L-**2** | **La-7** | 100/100 | 2 h/10 h | 100/74.0 | 72.1 (65.8) | 1.03 (1.03) |

[a] Polymerization conditions: [La]/[**Mn-1**] = 1/1 at −35 °C in a glovebox. [b] Monomer conversion (Conv.) was determined from the intensity of the Fourier transform infrared peak at 1805 $cm^{-1}$, which corresponds to the anhydride group of the OCA. [c] Determined by SEC. $M_n$-b1 and $Đ$-b1 refer to the $M_n$ and $Đ$ values of the first block polymer. The cyclic topologies of the obtained polymers and block copolymers were also verified; see Figures 3A–C, S8-S10, S17, and S18. [d] Copolymerization was performed at −15 °C.

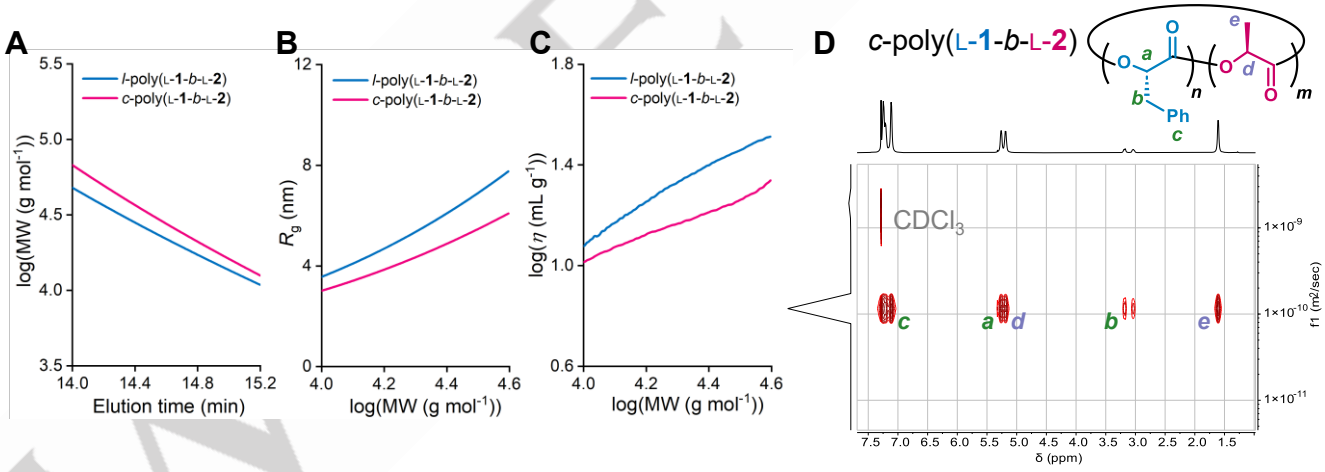


**Figure 3**. Characterization data for cyclic block copolyester *c*-poly(L-**1**-*b*-L-**2**). (A) Plots of log MW versus SEC elution time, (B) plots of $R_g$ versus log MW, and (C) Mark–Houwink–Sakurada plots of log $\eta$ versus log MW for *l*- and *c*-poly(L-**1**-*b*-L-**2**), as determined by SEC. (D) Diffusion-ordered NMR spectrum (DOSY) of *c*-poly(L-**1**-*b*-L-**2**) ($^1$H, $^{13}$C, and DOSY NMR spectra of corresponding homopolymers, *c*-poly(L-**1**) and *c*-poly(L-**2**), are shown in Figure S12).

## Preparation of Cyclic Block PAHAs

The living nature of our La/Mn-mediated polymerization for cyclic polyester synthesis prompted us to investigate whether cyclic block copolyesters could be prepared via sequential addition of monomers. Indeed, cyclic diblock copolymers could be readily prepared in one pot by sequential addition of L-**1**/L-**2**, L-**1**/ L-**4**, and L-**2**/L-**4** monomer pairs; and remarkable control of $M_n$ and $Đ$ was achieved (Table 2, entries 4–8; Figures S12–S16). Note that the monomer for the second block was added immediately following the complete consumption of the first block's monomer in order to leverage the active lanthanum species for continuous enchainment. SEC measurements of *dn*/*dc*, elution time, $R_g$, and $\eta$ showed that the obtained block copolyesters (e.g., *c*-poly(L-**1**-*b*-

L-**2**)) had cyclic rather than linear topologies (Figure 3A–C; SEC data for the other block copolyesters are shown in Figures S17 and S18). Additionally, the diffusion-ordered spectroscopy NMR data of all the block copolyesters showed a single diffusion coefficient for all resonances, which confirmed the formation of block copolymers (see Figure 3D and Figure S12 for *c*-poly(L-**1**-*b*-L-**2**) and Figures S14, and S16 for other block copolyesters). Notably, the diffusion coefficient ($f_1$) of *c*-poly(L-**1**-*b*-L-**2**) was approximately an order of magnitude lower than that of either *c*-poly(L-**1**) or *c*-poly(L-**2**) (Figure S12d), suggesting that the cyclic block copolymer was the only product and no homopolymer remained after the reaction. Furthermore, NMR studies showed no epimerization of the α-methine hydrogen atom (Figures S12–S16), and all of the obtained cyclic block PAHAs had highly ordered microstructures, as evidenced by the well-defined methine peaks at 5.2 ppm (Figure S12-16). In comparison, the cooresponding random (*r*) copolymer *c*-poly(L-**1**-*r*-L-**2**), *c*-poly(L-**1**-*r*-L-**4**) and *c*-poly(L-**2**-*r*-L-**4**) showed broad peaks in this region (Figure S19).

Noticably, the cyclic block copolymers *c*-poly(L-**1**-*b*-L-**2**) and *c*-poly(L-**2**-*b*-L-**4**) exhibited distinctive $T_g$ and $T_m$ values (Figure S20a, c), which were different from those of blended homopolymers (i.e., *c*-poly(L-**1**) + *c*-poly(L-**2**), *c*-poly(L-**2**) + *c*-poly(L-**4**), respectively) and those of random copolymers (*c*-poly(L-**1**-*r*-L-**2**) and *c*-poly(L-**2**-*r*-L-**4**). Notably, both random copolymer (*c*-poly(L-**1**-*r*-L-**2**) and *c*-poly(L-**2**-*r*-L-**4**) did not exhibit $T_m$ peaks in DSC. Moreover, *c*-poly(L-**1**-*b*-L-**4**) showed a $T_g$ of 25.1 °C (Figure S20b), which is between the $T_g$ values for *c*-poly(L-**1**) (43.1 °C) and *c*-poly(L-**4**) (11.8 °C). However, the blended *c*-poly(L-**1**) and *c*-poly(L-**4**) showed only one $T_g$ peak in DSC (46.5 °C). These DSC results, together with the well-splitted peaks in NMR spectra (Figures S12-16 versus Figure S19), confirmed the block microstructure of our synthesized cyclic PAHA copolymers.

## Assessment of Mechanical Properties of Cyclic PAHAs

We next turned our attention to assessing the mechanical properties of cyclic PAHAs' mechanical properties and comparing to corresponding linear PAHAs. Cyclic *c*-poly(L-**1**) ($M_n$ = 76.4 kDa) exhibited a fracture strength (σ) of 12.3 MPa and a fracture strain (Ɛ) of 29.5 %, achieving 1.2-fold higher toughness compared to *l*-poly(L-**1**) ($M_n$ = 48.2 kDa; Figure 4). Both *c*-poly(L-**2**) and *c*-poly(L-**3**) retained brittle characteristics in the tensile tests (Ɛ < 1%), similar to their linear counterparts. Noticeably, the stereocomplex polymer *c*-poly(*sc*-**1**) showed increased strength (σ = 14.9 MPa) and better ductility (Ɛ = 33.7 %) relative to *c*-poly(L-**1**) (Figure 4). Additionally, *c*-poly(L-**4**) displayed 3.6-times enhanced toughness compared to linear *l*-poly(L-**4**) (Figure S20d). Furthermore, the cyclic block copolymer *c*-poly(L-**1**-*b*-L-**4**), which comprising glassy block poly(L-**1**) and soft block poly(L-**4**), displayed an increased σ of 7.9 MPa compared to the linear MW-matched *l*-poly(L-**1**-*b*-L-**4**); and such cyclic block copolymer had a decent Ɛ of 231% (Figure 4, detailed MWs and phase-transition temperatures in Table S8).

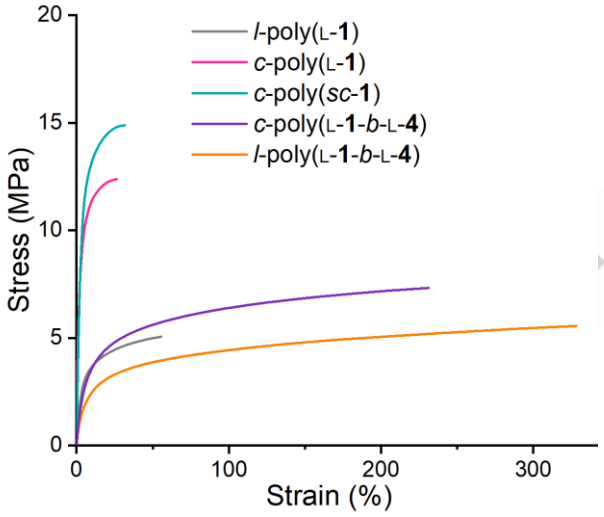


**Figure 4**. Representative stress–strain curves obtained by uniaxial extension of various linear and cyclic PAHA homopolymers and block copolymers. Polymer MWs, *Đ*s, and phase-transition temperatures are provided in Table S8.

## Degradation of Cyclic PAHAs

Linear PAHAs can be recycled via enzymatic or chemical degradation.[23] Although *l*-poly(L-**1**) could be degraded to the corresponding methyl ester by treatment with $Zn[N(SiMe_3)_2]_2$ in MeOH at 50 °C, a higher temperature (65 °C) was required for complete degradation of *c*-poly(L-**1**) (Scheme 2, Figure S21), presumably because the cyclic polymer lacks a chain end. After filtering off the insoluble zinc complex, we readily recovered the corresponding enantiopure methyl ester in quantitative yield by evaporation of the filtrate. This method could be extended to *c*-poly(L-**2**), which could be completely degraded to the corresponding methyl ester at 65°C (Figure S22). The obtained methyl esters could be rapidly converted to the corresponding α-hydroxy acids by means of our previously described method,[23] thereby closing the recycling loop.

**Scheme 2**. Efficient degradation of cyclic PAHAs to α-hydroxy acids.

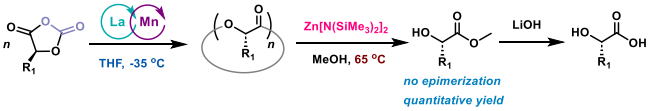

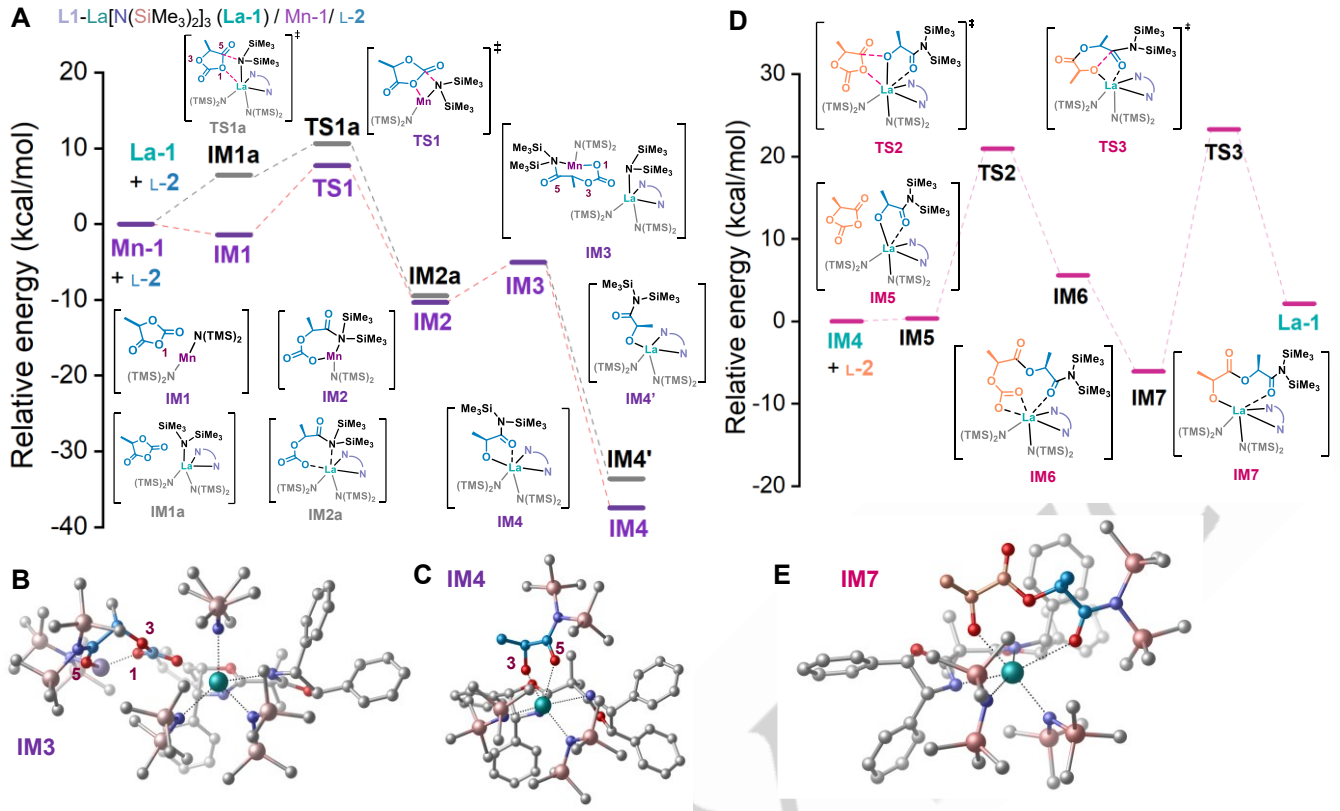


**Figure 5.** Proposed mechanism for ROP of OCAs to produce cyclic polyesters. (A) Free energy profile of proposed mechanism of initiation of **Mn-1**/**La-1**/L-**2** polymerization, calculated by means of density functional theory. (B,C) Three-dimensional structures of **IM3** (B) and **IM4** (C). (D) Free energy profile of proposed mechanism of propagation of **La-1**/L-**2** polymerization, in which a second L-**2** monomer reacts with **IM4**. (E) Three-dimensional structure of metallacycle **IM7**. Hydrogen atoms were omitted from the three-dimensional structural representations for clarity of visualization.

## Mechanistic Studies

We sought to elucidate the reason for the remarkably beneficial effect of using the bis(oxazoline) ligand of **La-1** for production of cyclic polyesters. Electrospray ionization mass spectrometric analysis of a 1/1 L-**1**/**La-1** mixture revealed that ligand **Ln-1** is bound to the lanthanum atom when the complex inserts into L-**1** (Figure S23). We then performed density functional theory (DFT) calculation on the initiation stage of the L-**2**/**La-1** polymerization (at the $SMD_{THF}$/ωB97M-V/def2-TZVP//PBE0-D3/6-31G(d) [MWB46(La), LANL2DZ(Mn)] level of theory, Figure 5A). Note that the DFT calculation of systems including **La-1** and **Mn-1** presented significant computational challenges, primarily due to the open-shell electronic configuration of manganese and the difficulty in achieving self-consistent field (SCF) convergence in such large molecular systems (over 200 atoms). Our previous studies revealed that **Mn-1** initiates the catalytic cycle through OCA ring-opening, followed by decarboxylation and transmetalation to generate metal-alkoxide species for enchainment.[23] Indeed, DFT computation showed the thermodynamic preference for L-**2** ring-opening by **Mn-1** (**TS1**) over **La-1** (**IM1a to TS1a**, free energy profile of ring-opening of L-**2** by **La-1** alone in Figure S24a). Since **Mn-1** alone had limited catalytic efficiency for enchainment (Table 1, entry 4), the cyclic manganese complex could adopt a skewed perpendicular orientation relative to the ligand plane when approaching the lanthanum atom in **La-1** (**IM3**, Figure 5B). The subsequent formation of cyclic lanthanum intermediate **IM4** proceeds via thermodynamically favorable irreversible decarboxylation and transmetalation steps. Notably, in this geometry, O3 and O5 of L-**2** are positioned 2.34 and 2.69 Å, respectively, from the lanthanum center (Figure 5C), forming a metallacycle. In contrast, the linear conformation of ring-opened L-**2** in intermediate **IM4'** exhibits an energy that is 3.84 kcal/mol higher than that of the metallacycle. The stability of the metallacycle and the steric bulk of the ligand might prevent abstraction of an α-hydrogen by the lanthanum atom, which could result in epimerization.

Our chain propagation analysis focused specifically on ligand effects during enchainment (Figure 5D). **Mn-1** was not included for the DFT computation based on two key considerations: its role is limited to lowering the activation barrier for OCA ring-opening and acclerating decarboxylation kinetics,[23] and its inclusion would significantly increase DFT computational complexity as mentioned above. For the new propagating lanthanum metallacycle **IM5,** transition state **TS2** is formed via nucleophilic attack of a lanthanum alkoxide at the C5 carbonyl of L-**2** followed by decarboxylation to form a metallacycle (Figure 5E). Importantly, the energy barrier for cyclization (**IM7** to **TS3**, 29.37 kcal/mol, Figure 5D) was substantially higher than that for monomer insertion (**IM5** to **TS2,** 20.60 kcal/mol), indicating that the

cyclization would not occur until all monomer was consumed up, agreeing well with the experimental results (Figure S5e, $Đ < 1.2$ over the course of polymerization). On the other hand, DFT computation of the chain propagation of L-**2**/La[N(SiMe$_3$)$_2$]$_3$ showed that the cyclization process could be thermodynamically favorable for the lanthanum complex without ligand (Figure S24d). Taken together, these results reveal that networks of attractive interaction involving the lanthanum alkoxide and the trimethylsilyl amide, aided by the rigid catalyst ligand scaffold, help stabilize the putative cyclic structure and orient the enchainment in a controlled manner. Our DFT calculations thus support our hypothesis of employing sterically confined ligands for lanthanum complex to facilitate enchainment while minimizing side reactions (Scheme 1B).

## Conclusion

In polymer chemistry, ligands for metal complex are often employed to control polymer stereochemistry. Herein, utilizing sterically confined ligands for lanthanum complexes have been shown to effectively hold the end of the growing cyclic polymers while catalyzing the continued addition of monomers and mitigating undesired side reactions, representing a powerful strategy for producing cyclic polymers (Scheme 1). Non-intuitively, in our synthesis of cyclic PAHAs, incorporating ligands to the lanthanum complex does not lower the polymerization rates (Table 1, entries 1 versus 5). Instead, the polymerization exhibited living characteristics (Figure 2E, Figures S5e and S6e), with MWs linearly increasing based on the monomer-to-catalyst feed ratios (Figure 2D). This living polymerization enables the unprecedented synthesis of cyclic block PAHAs, highlighting the effectiveness of our ligand strategy in cyclic polymer synthesis, which diverges from conventional use of ligands in cyclic polymer synthesis. The obtained cyclic PAHAs display distinctive physicochemical properties, including elevated $T_g$ and $T_m$ values (Figures S11 and S20), reduced viscosity, and enhanced mechanical toughness (Figure 4), compared to their linear analogues. The unique properties of cyclic block PAHAs are poised to offer opportunities for applying such new degradable polyester materials, particularly in biomedical engineering where high mechanical strength and processability are essential for degradable implants or sutures, and in drug delivery systems where the cyclic topology facilitates extended circulation half-lives.[26]

## Supporting Information

The authors have cited additional references within the Supporting Information. [27]

## Acknowledgements

We thank Dr. N. Murthy Shanaiah and Ken Sharp-Knott (Department of Chemistry, Virginia Tech) for NMR spectroscopy experiments, and Dr. Keith Ray (Department of Biochemistry, Virginia Tech) for matrix-assisted laser desorption/ionization mass spectrometry measurements.

**Keywords:** cyclic polyester• ring-opening polymerization • poly(α-hydroxy acid) • *O*-carboxyanhydride • cyclic block copolyester

[1] a) Y. Tezuka, H. Oike, *Prog. Polym. Sci.* **2002**, *27*, 1069-1122; b) T. Yamamoto, Y. Tezuka, *Polym. Chem.* **2011**, *2*, 1930-1941.

[2] a) J. A. Semlyen, *Cyclic polymers*, *2nd ed*.; Kluwer Academic Publishers: Dordrecht, the Netherlands, **2000**; b) K. Endo, in *New Frontiers in Polymer Synthesis* (Eds.: S. Kobayashi), Springer Berlin Heidelberg, Berlin, Heidelberg, **2008**, pp. 121-183; c) F. M. Haque, S. M. Grayson, *Nat. Chem.* **2020**, *12*, 433-444; d) M. Kapnistos, M. Lang, D. Vlassopoulos, W. Pyckhout-Hintzen, D. Richter, D. Cho, T. Chang, M. Rubinstein, *Nat. Mater.* **2008**, *7*, 997-1002; e) J. Roovers, P. M. Toporowski, *Macromolecules* **1983**, *16*, 843-849.

[3] B. A. Laurent, S. M. Grayson, *Chem. Soc. Rev.* **2009**, *38*, 2202-2213.

[4] a) C. W. Bielawski, D. Benitez, R. H. Grubbs, *Science* **2002**, *297*, 2041-2044; b) Y. Xia, A. J. Boydston, Y. Yao, J. A. Kornfield, I. A. Gorodetskaya, H. W. Spiess, R. H. Grubbs, *J. Am. Chem. Soc.* **2009**, *131*, 2670-2677.

[5] a) M. L. McGraw, R. W. Clarke, E. Y. X. Chen, *J. Am. Chem. Soc.* **2021**, *143*, 3318-3322; b) Y. Song, J. He, Y. Zhang, R. A. Gilsdorf, E. Y. X. Chen, *Nat. Chem.* **2023**, *15*, 366-376.

[6] a) K.-Y. Yoon, J. Noh, Q. Gan, J. P. Edwards, R. Tuba, T.-L. Choi, R. H. Grubbs, *Nat. Chem.* **2022**, *14*, 1242-1248; b) Z. Miao, S. A. Gonsales, C. Ehm, F. Mentink-Vigier, C. R. Bowers, B. S. Sumerlin, A. S. Veige, *Nat. Chem.* **2021**, *13*, 792-799.

[7] a) Y. A. Chang, R. M. Waymouth, *J. Polym. Sci. A Polym. Chem.* **2017**, *55*, 2892-2902; b) H. R. Kricheldorf, *J. Polym. Sci. A Polym. Chem.* **2010**, *48*, 251-284.

[8] a) Y. Zhu, C. Romain, C. K. Williams, *Nature* **2016**, *540*, 354-362; b) R. Tong, *Ind. Eng. Chem. Res.* **2017**, *56*, 4207-4219; c) X. Tang, E. Y. X. Chen, *Chem* **2019**, *5*, 284-312; d) A. L. Chin, X. Wang, R. Tong, *Macromol. Biosci.* **2021**, *21*, 2100087; e) J. N. Hoskins, S. M. Grayson, *Polym. Chem.* **2011**, *2*, 289-299; f) P. B. Yang, M. G. Davidson, K. J. Edler, S. Brown, *Biomacromolecules* **2021**, *22*, 3649-3667.

[9] H. A. Brown, R. M. Waymouth, *Acc. Chem. Res.* **2013**, *46*, 2585-2596.

[10] a) H. R. Kricheldorf, S. M. Weidner, *Eur. Polym. J.* **2018**, *105*, 158-166; b) H. R. Kricheldorf, S. M. Weidner, A. Meyer, *Polym. Chem.* **2020**, *11*, 2182-2193; c) C. Hu, E. Louisy, G. Fontaine, F. Bonnet, *J. Polym. Sci. A Polym. Chem.* **2017**, *55*, 3175-3179; d) J. Weil, R. T. Mathers, Y. D. Y. L. Getzler, *Macromolecules* **2012**, *45*, 1118-1121; e) F. Bonnet, F. Stoffelbach, G. Fontaine, S. Bourbigot, *RSC Adv.* **2015**, *5*, 31303-31310.

[11] L. Zhou, L. T. Reilly, C. Shi, E. C. Quinn, E. Y. X. Chen, *Nat. Chem.* **2024**, *16*, 1357-1365.

[12] a) H. R. Kricheldorf, N. Lomadze, G. Schwarz, *Macromolecules* **2008**, *41*, 7812-7816; b) Y. Wang, T.-Q. Xu, *Macromolecules* **2020**, *53*, 8829-8836.

[13] a) H. R. Kricheldorf, S. M. Weidner, *Polym. Chem.* **2020**, *11*, 5249-5260; b) P. Piromjitpong, P. Ratanapanee, W. Thumrongpatanaraks, P. Kongsaeree, K. Phomphrai, *Dalton Trans.* **2012**, *41*, 12704-12710; c) P. Wongmahasirikun, P. Prom-on, P. Sangtrirutnugul, P. Kongsaeree, K. Phomphrai, *Dalton Trans.* **2015**, *44*, 12357-12364; d) H. R. Kricheldorf, S. M. Weidner, F. Scheliga, *Eur. Polym. J.* **2019**, *116*, 256-264.

[14] R. W. F. Kerr, P. M. D. A. Ewing, S. K. Raman, A. D. Smith, C. K. Williams, P. L. Arnold, *ACS Catal.* **2021**, *11*, 1563-1569.

[15] C. Goonesinghe, H.-J. Jung, H. Roshandel, C. Diaz, H. A. Baalbaki, K. Nyamayaro, M. Ezhova, K. Hosseini, P. Mehrkhodavandi, *ACS Catal.* **2022**, *12*, 7677-7686.

[16] a) Q. Yin, L. Yin, H. Wang, J. Cheng, *Acc. Chem. Res.* **2015**, *48*, 1777-1787; b) X. Wang, A. L. Chin, R. Tong, *Org. Mater.* **2021**, *03*, 041-050.

[17] J. Liang, T. Yin, S. Han, J. Yang, *Polym. Chem.* **2020**, *11*, 6944-6952.

[18] E. Piedra-Arroni, C. Ladavière, A. Amgoune, D. Bourissou, *J. Am. Chem. Soc.* **2013**, *135*, 13306-13309.

[19] a) X. Wang, Z. Huo, X. Xie, N. Shanaiah, R. Tong, *Chem. Asian J.* **2023**, *18*, e202201147; b) X. Xie, Z. Huo, E. Jang, R. Tong, *Commun. Chem.* **2023**, *6*, 202.

[20] a) M. Hong, E. Y. X. Chen, *Nat Chem* **2016**, *8*, 42-49; b) J.-B. Zhu, E. M. Watson, J. Tang, E. Y.-X. Chen, *Science* **2018**, *360*, 398-403.

[21] R. Wang, J. Zhang, Q. Yin, Y. Xu, J. Cheng, R. Tong, *Angew. Chem. Int. Ed.* **2016**, *55*, 13010-13014.

[22] G. W. Coates, *Chem. Rev.* **2000**, *100*, 1223-1252.

[23] X. Wang, A. L. Chin, J. Zhou, H. Wang, R. Tong, J. Am. Chem. Soc. 2021, 143, 16813-16823.

[24] H. Wang, H. Ma, *Macromolecules* **2024**, *57*, 6156-6165.

[25] H. Li, J. Ollivier, S. M. Guillaume, J.-F. Carpentier, *Angew. Chem. Int. Ed.* **2022**, *61*, e202202386.

[26] N. Nasongkla, B. Chen, N. Macaraeg, M. E. Fox, J. M. J. Fréchet, F. C. Szoka, *J. Am. Chem. Soc.* **2009**, *131*, 3842-3843.

[27] a) Q. Yin, R. Tong, Y. Xu, L. W. Dobrucki, T. M. Fan, J. Cheng, *Biomacromolecules* **2013**, *14*, 920-929; b) O. Thillaye du Boullay, E. Marchal, B. Martin-Vaca, F. P. Cossío, D. Bourissou, *J. Am. Chem. Soc.* **2006**, *128*, 16442-16443; c) A. Buchard, D. R. Carbery, M. G. Davidson, P. K. Ivanova, B. J. Jeffery, G. I. Kociok-Köhn, J. P. Lowe, *Angew. Chem. Int. Ed.* **2014**, *53*, 13858-13861; d) Y. Lu, L. Yin, Y. Zhang, Z. Zhang, Y. Xu, R. Tong, J. Cheng, *ACS Macro Lett.* **2012**, *1*, 441-444; e) S. A. Schuetz, V. W. Day, R. D. Sommer, A. L. Rheingold, J. A. Belot, *Inorg. Chem.* **2001**, *40*, 5292-5295; f) R. Anwander, O. Runte, J. Eppinger, G. Gerstberger, E. Herdtweck, M. Spiegler, *J. Chem. Soc., Dalton Trans.* **1998**, 847-858; g) S. Hong, S. Tian, M. V. Metz, T. J. Marks, *J. Am. Chem. Soc.* **2003**, *125*, 14768-14783; h) R. A. Andersen, K. Faegri, Jr., J. C. Green, A. Haaland, M. F. Lappert, W. P. Leung, K. Rypdal, *Inorg. Chem.* **1988**, *27*, 1782-1786; i) D.-Y. Lee, J. F. Hartwig, *Org. Lett.* **2005**, *7*, 1169-1172; j) D. C. Bradley, J. S. Ghotra, F. A. Hart, *J. Chem. Soc. Dalton Trans.* **1973**, 1021-1023; k) A. R. Smith, T. Livinghouse, *Organometallics* **2013**, *32*, 1528-1530; l) C. A. Tolman, *Chem. Rev.* **1977**, *77*, 313-348; m) D. J. Durand, N. Fey, *Chem. Rev.* **2019**, *119*, 6561-6594; n) I. A. Guzei, M. Wendt, *Dalton Trans.* **2006**, 3991-3999; o) R. Pollice, P. Chen, *Angew. Chem. Int. Ed.* **2019**, *58*, 9758-9769; p) X. Wang, Y. Huang, X. Xie, Y. Liu, Z. Huo, M. Lin, H. Xin, R. Tong, *Nat. Commun.* **2023**, *14*, 3647; q) M. Frisch, G. Trucks, H. Schlegel, G. Scuseria, M. Robb, J. Cheeseman, G. Scalmani, V. Barone, G. Petersson, H. Nakatsuji, Gaussian, Inc. Wallingford, CT, **2016**; r) S. Grimme, J. Antony, S. Ehrlich, H. Krieg, *J. Chem. Phys.* **2010**, *132*, 154104; s) J. P. Perdew, K. Burke, M. Ernzerhof, *Phys. Rev. Lett.* **1996**, *77*, 3865-3868; t) C. Adamo, V. Barone, *J. Chem. Phys.* **1999**, *110*, 6158-6170; u) M. Ernzerhof, G. E. Scuseria, *J. Chem. Phys.* **1999**, *110*, 5029-5036; v) M. Dolg, H. Stoll, A. Savin, H. Preuss, *Theo. Chim. Acta* **1989**, *75*, 173-194; w) L. E. Roy, P. J. Hay, R. L. Martin, *J. Chem. Theory Comput.* **2008**, *4*, 1029-1031; x) F. Neese, *WIREs Comput. Mol. Sci.* **2012**, *2*, 73-78; y) F. Neese, *WIREs Comput. Mol. Sci.* **2022**, e1606; z) N. Mardirossian, M. Head-Gordon, *J. Chem. Phys.* **2016**, *144*, 214110; aa) F. Weigend, *Phys. Chem. Chem. Phys.* **2006**, *8*, 1057-1065; ab) A. V. Marenich, C. J. Cramer, D. G. Truhlar, *J. Chem. Phys. B* **2009**, *113*, 6378-6396; ac) B. Chan, P. M. W. Gill, M. Kimura, *J. Chem. Theo. Comput.* **2019**, *15*, 3610-3622; ad) T. Lu, Q. Chen, *Comput. Theo. Chem.* **2021**, *1200*, 113249; ae) A. P. Scott, L. Radom, *J. Phys. Chem.* **1996**, *100*, 16502-16513; af) C. Legault, *CYLview, 1.0 b, Vol. 436*, Université de Sherbrooke, **2009**.

## Entry for the Table of Contents

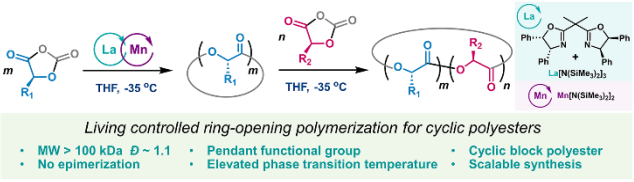


A novel catalytic system consisting of a lanthanum complex with a sterically bulky ligand and a manganese silylamide has been developed to prepare high-molecular-weight (> 100 kDa) stereoregular cyclic polyesters and block copolyesters with narrow molecular weight distributions (*Đ* < 1.1) and unique physical properties.